Indian Journal of Chemistry
Vol. 60A, July 2021, pp. 953-958

Synthesis and characterisation of nickel-iron bimetallic oxide nanoparticles via microwave irradiation technique

V G Viju Kumar*, Vidya V G & Arsha P Mohan

Department of Chemistry, University College, Thiruvananthapuram 695 034, India

*E-mail: viju@universitycollege.ac.in

Received 22 September 2020; revised and accepted 01 May 2021

Nickel- Iron bimetallic oxide nanoparticles have been synthesized in ethylene glycol using microwave irradiation technique. The microwave assisted synthesized Nickel and iron oxide nanoparticles are combined together in 1:1 molar ratio and treated under microwave irradiation followed by calcination to get Ni-Fe bimetallic oxide. The structure and composition of nanoparticles are characterized by UV-visible spectroscopy, FT-IR, X-ray diffraction (XRD), energy dispersion spectroscopy (EDS) and transmission electron microscopy (TEM) techniques. The empirical formula of the nanoparticle is found as $Ni_1Fe_{1.6}O_{2.9}$ at 500 ºC, $Ni_1Fe_{1.5}O_{2.6}$ at 700 ºC and $Ni_1Fe_2O_{2.7}$ at 900 ºC by varied reaction conditions. A maximum absorbance of 357.67 nm is observed in UV-visible spectrum. The average size of particles in all cases is found to be ~30 nm as confirmed from TEM images. Antibacterial and antifungal studies have not shown any appreciable results.

Keywords: Bimetallic oxide nanoparticle, Nickel- Iron, Microwave irradiation, Green synthesis

Metal oxide based nanomaterials are employed in the manufacture of photocells, transistors, diodes, sensors, catalysts and abundantly used in optoelectronics and photonics devices[1]. Various nanomaterials are employed in effective energy production, removal of pollutants, and environmental protection[2]. Being ecofriendly, simple, stable, rapid and cost effective, green synthesis provides a new scope for nanoparticle (NP) synthesis. The nanostructured materials are very interesting materials both for scientific reasons and practical applications[3-10]. Last two decades of scientific research draws considerable interest in bimetallic NP system rather than monometallic NPs. Bimetallic systems can be carbon supported, graphene supported or other inorganic materials like zeolite supported nanocomposites which displays wide array of applications. For treating chlorinated organic pollutants, iron based bimetallic NPs can be effectively used. By varying the stoichiometric ratio of metals in bimetallic system based on nickel, the catalytic properties can be modified[11]. If the grain size in the range of 30-50 nm, Fe based bimetallic nano alloy tend to show promising catalytic activity for dechlorinating chlorinated methane systems[12]. Recently, bimetallic NPs are found to exhibit antibacterial properties surpassing that of monometallic counterparts owing to synergistic effects. Several bimetallic systems such as Pd- Fe, Pt- Co, Ru- Co, Pt- Au, Pd- Au are well studied where an inert metal is used as an inert carrier along with an active counterpart[13]. The study is of worth noticing because of the increased potential application for which they can be applied, mainly in industrial catalytic applications. The advantage of bimetallic oxide NPs over monometallic oxide is that they incorporate nanoscale properties of more than one element within one NP. Thereby enhance the properties through synergetic interaction between those elements. The union of two active metallic elements is promising as catalytic candidate such as Ni-Fe bimetallic oxide which can show enhanced properties of both the metals[13].

NPs can be synthesized by different methods such as hydrothermal synthesis, microwave irradiation, CVD, green synthesis, sol-gel, solvothermal method, combustion, templating, sputtering etc.[12]. Nickel iron oxide NPs find applications in levitated railway systems, solid oxide fuel cells, magnetic refrigeration, microwave absorbers, lithium ion micro batteries, electrochromic coatings, plastics and textiles, in nanowires, nanofibers and in catalytic systems. In this work, we consider the microwave assisted green synthesis of Nickel-Iron bimetallic oxide by polyol method using ethylene glycol as solvent, hydrazenium hydroxide as reducing agent and poly vinyl

pyrrolidone (PVP) as capping agent. It is a time and energy saving method compared to the conventional methods as it takes several minutes to complete the reaction using microwave irradiation whereas conventional procedures take several hours. Polyol synthesis is the most convenient method for the synthesis of metal oxide NPs of uniform size due to high boiling point and penetration power[14]. Nickel-Iron bimetallic oxide possesses localized surface plasmon resonance (SPR) properties and optical properties[15-16]. Here we consider the synthesis of Ni-Fe bimetallic oxide in the ratio 1:2 and study the variation of particle size and stoichiometric ratio with respect to the calcination temperature. Characterization were done by using UV-visible spectroscopy, FT-IR, X-ray diffraction (XRD), energy dispersion spectroscopy (EDS) and transmission electron microscopy (TEM) techniques

Materials and Methods

The chemicals such as $Fe(NO_3)_2.9H_2O$, Urea, $NiCl_2.6H_2O$, ethylene glycol, PVP, Na_2CO_3, hydrazenium hydroxide and NaOH (Merck or Fluka) used here are of AR grade. The instruments used in the present investigation are Electrolux MX21WF spectra-900 W domestic microwave oven, Schimadzu UV 2450, Schimadzu DR-43S FT-IR spectrophotometer, Carl Zeiss EVO 18 secondary electron microscope with EDS, Bruker D8 Advance X-ray diffractometer and Joel/JEM 2100 LaB6 high resolution transmission electron microscope.

Synthesis of Ni nanoparticles

The Ni NPs were synthesized by polyol method using microwave irradiation, which is based on the principle of precipitation of metal ions in solution in the presence of a capping agent. 5 mL of 1 M $NiCl_2$ solution was mixed with 1 mL of 0.1 M Na_2CO_3 solution, 4 mL of PVP solution, 0.2 mL of 0.1 M NaOH solution and 0.6 mL of hydrazinium hydroxide ($N_2H_4.H_2O$) solution in a flask. Ethylene glycol was added to keep the volume of the mixture fixed to 20 mL. The mixture solution was irradiated under microwave in a domestic microwave oven for 120 s. The obtained colloidal solution of Ni NPs was transferred to an ice bath to prevent agglomeration. The precipitate was filtered and dried in air oven at 200 ºC for 30 min[17].

Synthesis of iron oxide nanoparticles

In order to prepare α-Fe_2O_3 (hematite) NPs as the starting materials, a mixed solution of 50 mL of 0.3 M $Fe(NO_3)_2.9H_2O$ and 1.2 g of urea was irradiated under 540 W microwave for 6 min. The precipitate was filtered, washed with deionised distilled water and dried in an oven at 100 ºC for 8 h to obtain the solid sample. Then, the as prepared sample was calcined at 800 ºC for 4 h to obtain the brown species[18].

Synthesis of bimetallic oxide nanoparticles

The procedure of synthesis of bimetallic oxide[19] is already reported and the same is employed here as shown in Scheme 1. 0.58 g Ni NPs were dispersed in 20 mL ethylene glycol and 0.67 g iron oxide NPs were added to it. To this, 4 mL PVP solution and 0.6 mL hydrazenium hydroxide were added. The mixture was irradiated in a microwave oven for 2-3 min until a dark coloured solution was obtained which was considered as the end of the reaction. The final product was filtered, washed with distilled water. Three different samples were calcined in a muffle furnace at 500 ºC, 700 ºC and 900 ºC for one hour, respectively. The intention of the work was to check whether the process will change the stoichiometric composition of resultant product and the effect of calcination on the grain size which was not reported earlier.

Results and Discussion

The absorption spectrum of nickel-iron oxide NPs was recorded in the range of 200-700 nm as shown Fig. 1. Here the maximum absorbance is observed at 357.67 nm. The peak may be due to d-d transitions of nickel. This is due to SPR on the surface of Ni NPs.

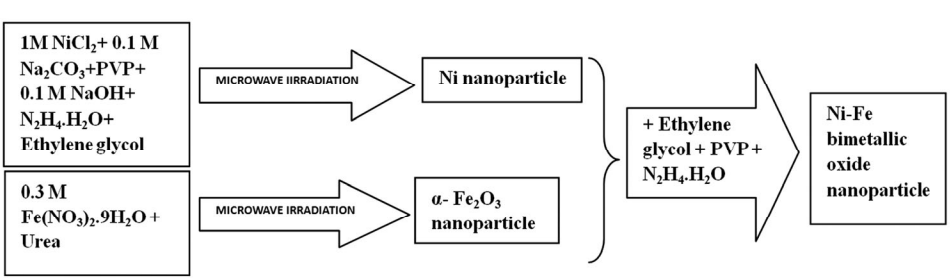

Scheme 1 — Schematic representation of the synthesis of Ni-Fe bimetallic oxide NPs

The unique optical properties of metal NPs are well known, the source of which is due to the collective coherent excitations of free electrons in a nano-sized metal, known as SPR [20].

The FT-IR spectrum of nickel iron oxide NPs showing IR absorption due to different vibrational modes is shown in the Fig. 2. Characteristic major peaks[21] are observed at 1606.70 cm^{-1}, 1381.03 cm^{-1}, 1352.10 cm^{-1}, 680.87cm^{-1} , 495.71 cm^{-1}, 453.27cm^{-1}, 412.77 cm^{-1}, 393.48 cm^{-1}. The broad absorption band in the region 600–700 cm^{-1} is assigned to Ni–O stretching vibration mode. The presence of NiO NPs is indicated by a peak[22] in the region 680.87cm^{-1}. The Fe-O-Fe stretching vibration is in the region 462 and 560 cm^{-1}. The presence of iron oxide NPs as it is indicated by a peak in the region 495.71 cm^{-1}. Also the observed bands below 500 cm^{-1} are due to

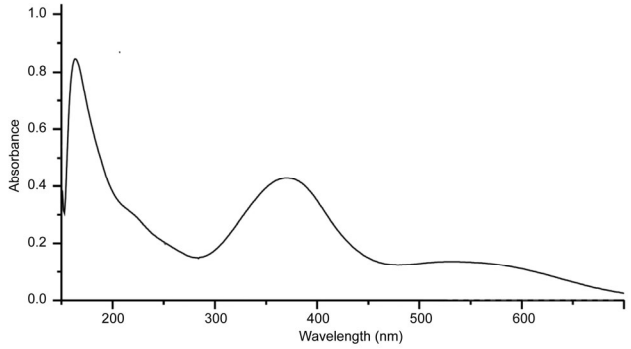

Fig. 1 — Absorption spectrum of Ni- Fe bimetallic oxide NPs

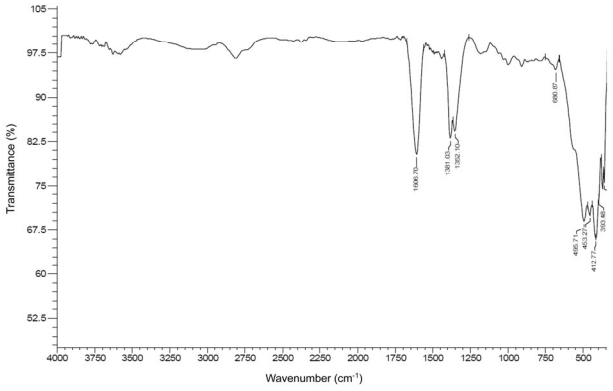

Fig. 2 — FT-IR spectrum of Ni-Fe bimetallic oxide NPs

vibrations of NiO_6 polyhedra[23]. The peaks at 680.87, 1352.10, 1381.03, 1606.70 cm^{-1} are due to Ni-Fe stretching. From the IR stretching frequencies the formation of iron nickel oxides can be proposed.

Electron diffraction studies were carried out using scanning electron microscope with EDS. The EDAX spectrum of nickel-iron oxide calcined at three different temperatures i.e.; 500 ºC, 700 ºC and 900 ºC is shown in Supplementary Data, Fig. S1. For sample calcined at 500 ºC, the average atomic weight percentage of Ni and Fe is about 30.45 and 45.76%, respectively. The elemental analysis confirms the presence of corresponding elements in their stoichiometric percentage. From the elemental mass analysis the expected empirical formula for the present compound was identified by dividing the weight percentage of element by atomic mass and multiplying with suitable number. By utilizing the above steps the empirical formula of our sample was found to be $Ni_1Fe_{1.6}O_{2.9}$. For sample calcined at 700 ºC, the average atomic weight percentage of Ni and Fe is found to be 32.13 and 45.56 %, respectively. The empirical formula of the sample is $Ni_1Fe_{1.5}O_{2.6}$. When calcined at 900 ºC, the average atomic weight percentage of Ni and Fe is about 27.83 and 51.74%, respectively. The elemental analysis is in accordance with the stoichiometric percentage. The empirical formula is obtained as $Ni_1Fe_2O_{2.7}$. The spectral data are presented in Table 1. As the temperature of calcination is increased to 900 ºC, an appreciable change in the stoichiometric composition is observed and Ni to Fe ratio became 1:2.

The XRD measurements were carried out using Brucker D8 Advance X-Ray diffractometer. The X-rays were produced using a sealed tube and the wavelength of X-Ray was 1.5406 Å. Fig. 3 shows powder XRD patterns for nickel iron oxide NPs prepared by microwave synthesis with PVP as capping agent and calcined at three different temperatures 500 ºC, 700 ºC and 900 ºC. The diffraction patterns produced by parent NiO was observed[24] at 37.3º, 43.4º and 62.9º by heating the sample (JCPDS file no. 22-1189). The main

Table 1 — EDS spectral Data

Element	500 ºC			700 ºC			900 ºC		
	Weight %	Atomic %	Error %	Weight %	Atomic %	Error %	Weight %	Atomic %	Error %
O	23.79	52.64	6.40	22.31	50.57	6.42	20.42	47.68	6.44
Fe	45.76	29.01	4.60	45.56	29.58	4.45	51.74	34.61	3.91
Ni	30.45	18.36	7.50	32.13	19.84	6.84	27.83	17.71	6.45

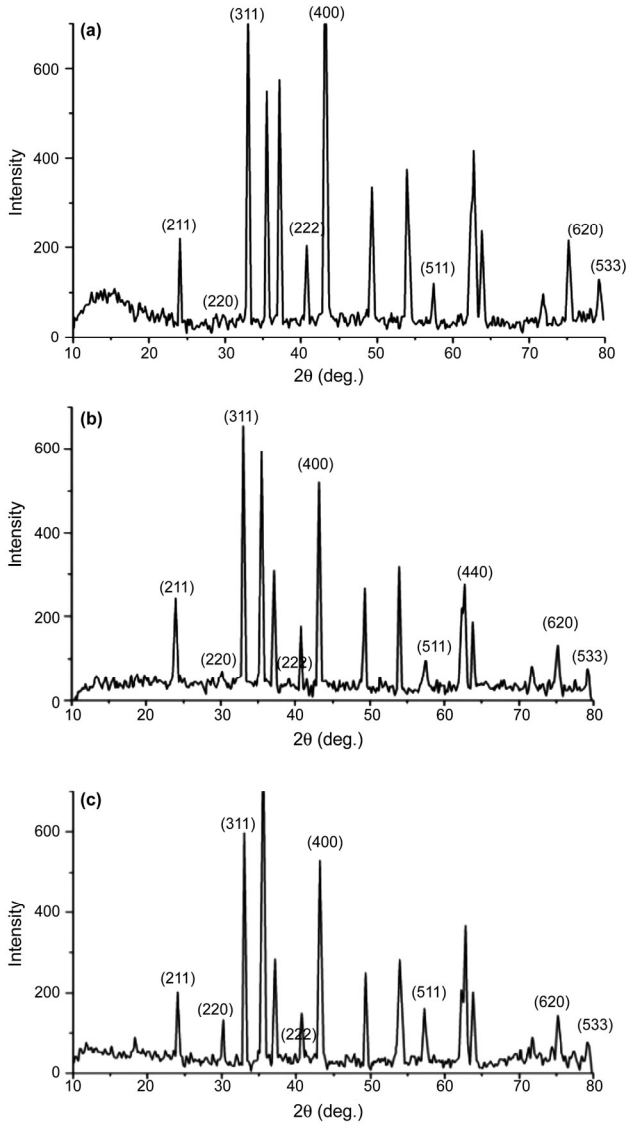

Fig. 3 — XRD patterns for nickel- iron oxide calcined at (a) 500, (b) 700 and (c) 900 ºC

diffraction peaks of iron oxide were observed at 30.103º, 35.451º, 43.088º, 53.516º, 56.998º, 62.657º and 74.098º (JCPDS file no. 65-3107). The size of nanocrystals were calculated using Debye Scherrer equation as follows,

$$A = K\lambda/(\beta cos\theta)$$

where, K is the shape factor constant taken as 0.9, λ is the wavelength of X-rays, β is the full width at half maximum in radians and θ is Bragg's angle. In the XRD patterns of nickel iron oxide calcined at 500 °C (Fig. 3a) besides strong peaks corresponding to FeO, new peaks at 33.055°, 35.517°, 37.155°, 43.184°, 49.345°, 53.961° and 62.742° are observed. Here 2θ is maximum at 43.184°. By using Debye Scherrer equation, the parameters are λ= 1.5406 Å, β= 4.76 x 10^{-3} rad; θ = 21.592. By substituting all these values in the equation, the crystallite size was obtained as 31.32 nm. In the XRD patterns of nickel-iron oxide calcined at 700 °C (Fig. 3b) besides strong peaks corresponding to FeO, new peaks at 24.020º, 33.033°, 35.509°, 37.124°, 43.151°, 49.325° and 53.949° are observed. In this 2θ is maximum at 33.033°. Here, λ= 1.5406 Å, β= 4.55 x 10^{-3} rad, θ =16.516°. By substituting all these values in the equation, the crystallite size was obtained as 31.78 nm. The XRD patterns of nickel iron oxide calcined at 900 °C (Fig. 3c) besides strong peaks of FeO, new peaks at 24.030°, 30.169°, 33.051°, 35.550°, 37.148°, 43.187° and 53.945° are observed. 2θ value is maximum at 35.550°. Employing Debye Scherrer equation, λ= 1.5406 Å; β= 4.67x10^{-3} rad; θ=17.775°, the crystallite size was obtained as 31.18 nm.

From XRD analysis, thus we can conclude that the average crystallite size of the NPs changes as the calcination temperature increases from 500 to 900 °C. The signals of Ni were not detected in the XRD pattern of NPs although the position and relative intensity of the diffraction peaks are reasonably close to the reported pattern[26,27]. The XRD pattern shows that the NPs are well-crystalline and exhibit diffraction peaks corresponding to (111), (220), (311), (400), (511) and (440) planes of a cubic crystal system. The XRD pattern indicates mixed phases of iron oxides with nickel[28].

Transmission electron microscope (TEM) is a type of electron microscope that produces image of the sample by scanning it with a focused beam of electrons. It gives us information about size and structure of particles. Fig. 4 shows the TEM micrographs of Nickel iron bimetallic oxide particles calcined at different temperatures There is slight agglomeration of the particles as shown Fig. 4a and 4d and most of the particles are spherical in shape. The average particle size of the NPs is found to be at 29 nm and 34 nm for samples calcinatied at 500 °C and 700 °C, respectively. This increase in particles size with increasing the calcinations temperature is in accordance with the results observed in the XRD measurements. The selected area diffraction patterns shown in Fig. 4c and 4e, show the diffraction due to different planes of cubic crystal structure.

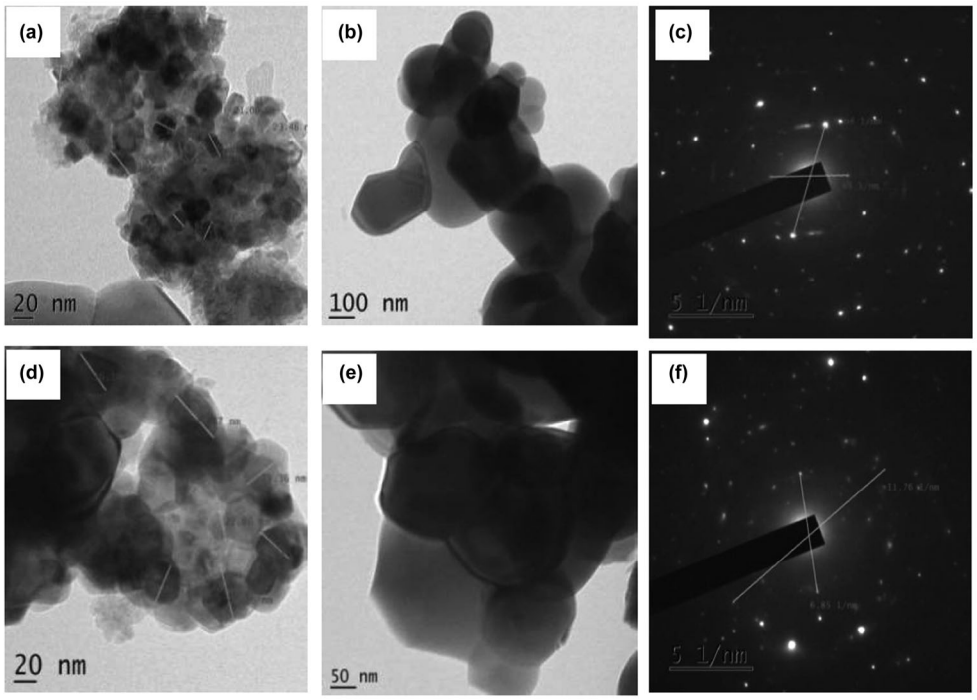

Fig. 4 — TEM images of Ni-Fe bimetallic oxide NPs calcined at (a, b) 500 °C and (d, e) 700 °C**.** The selected area diffraction patterns are shown in (c) for 500 °C and (e) for 700 °C

Antibacterial assay by agar well diffusion method

Antibactrial assay was done by Agar well diffusion method. 15-20 mL of Mueller-Hinton agar was poured on glass Petri plate and allowed to solidify. Wells with a diameter of 8 mm (20 mm apart from one another) were punched aseptically with a sterile cork borer in each plate. Standardized inoculums of the test organism were uniformly spread on the surface of these plates using sterile cotton swab. A volume (50 µL) of the extract solution at desired concentration was added to the wells and one well with Gentamycin maintained as positive and DMSO as a negative control. Then, the agar plates were incubated under suitable conditions depending upon the test microorganism. After incubation, clear zone was observed. Inhibition of bacterial growth was measured in mm. Mueller Hinton Agar M173 Himedia was used for determination of susceptibility of microorganisms to antimicrobial agents. Suspended 38 g in 1000 mL distilled water were heated to boiling to dissolve the medium completely followed by sterilization by autoclaving at 15 lbs pressure (121 °C) for 15 min. Then cooled to 45-50 °C, mixed well and poured into sterile Petri plates. Inoculums were procured from the microbial type culture collection and gene bank Chandigarh with MTCC No. 443. Incubation condition was 37 °C for 24 h. The data obtained is shown in Supplementary Data, Table S1. The picture of the culture was shown in Supplementary Data, Fig. S2a.

Antifungal assay by agar well diffusion method

For antifungal assay, 15-20 mL of Rose Bengal agar was poured on glass petri plates and allowed to solidify. Wells with a diameter of 8 mm (20 mm apart from one another) were punched aseptically with a sterile cork borer in each plate. Standardized inoculums of the test organism were uniformly spread on the surface of these plates using sterile cotton swab. A volume (50 µL) of the extract solution at desired concentration was added to the wells and one well with Clotrimazole maintained as positive and DMSO as a negative control. Then, the agar plates were incubated under suitable conditions depending upon the test microorganism. After incubation, clear zone was observed. Inhibition of the fungal growth was measured in mm. For culture medium, Rose Bengal agar M842 Himedia was used for determination of susceptibility of fungal strains to antifungal agents. 31.55 g was suspened in 1000 mL distilled water, heated to boiling to dissolve the medium completely, then sterilized by autoclaving at 15 lbs pressure (121 °C) for 15 min followed by cooling to 45-50 °C. Then it was mixed well and

poured into sterile Petri plates. Inoculums were procured from the microbial type culture collection and gene bank Chandigarh with MTTC No. 227. The data obtained is shown in Supplementary Data, Table S2. The picture of the culture was shown in Fig. S2b. Biological studies indicate that nickel iron bimetallic oxide NPs does not show any antibacterial and antifungal activities.

Conclusions

Ni-Fe bimetallic oxide NPs were successfully synthesized by microwave assisted polyol synthesis method in a fast, time saving and cost effective way. The composition and structure of NPs were characterized by TEM, EDS, FT-IR and XRD measurements. In FT-IR spectra, characteristic vibrations corresponds to NiO, Fe-O-Fe, Ni-Fe were observed, which indicate the formation of Ni-Fe bimetallic oxide NPs. The EDS study confirms the empirical formula of the sample formed at three different calcinations temperatures i.e., $Ni_1Fe_{1.6}O_{2.9}$, $Ni_1Fe_{1.5}O_{2.6}$ and $Ni_1Fe_2O_{2.7}$ at 500, 700 and 900 °C, respectively. As the calcination temperature increased to 900 °C, stoichiometric composition is varied and Ni to Fe ratio became 1:2. XRD analysis showed characteristic peaks of Ni-Fe bimetallic oxide and supports its formation and variation of average crystallite size with the calcinations temperature, which is further supported by the TEM results. Antibacterial and antifungal studies reveal that the NPs do not show any appreciable biological activities.

Supplementary Data

Supplementary data associated with this article are available in the electronic form at http://nopr.niscair.res.in/jinfo/ijca/IJCA_60A(07)953-958_SupplData.pdf.

Acknowledgement

The authors acknowledge the Department of Chemistry, University College, Thiruvananthapuram for the facility and support from STIC, Cochin, for use of their TEM facility.

References

1 Shaheen K, Shah Z, Asad A, Arshad T, Khan S B & Suo S, *ACS Omega,* 5 (2020) 15992.
2 Huynh K H, Pham X H, Kim J, Lee S H, Chang H, Rho W Y & Jun B H, *Int J Mol Sci,* 21 (2020) 5174.
3 Mandal G & Ganguly T, *Indian J Phys,* 85 (2011) 1229.
4 Inamdar A I, Lee S, Kim D, Gurav K V, Kim J H, Im H, Jung W & Kim H, *Thin Solid Films*, 537 (2013) 36.
5 Sarmah S & Kumar A, *Indian J Phys,* 85 (2011) 713.
6 Barman B & Sarma K C, *Indian J Phys,* 86 (2012) 703.
7 Tekerek S, Kudret A & Alver U, *Indian J Phys,* 85 (2011) 1469.
8 Pathak C S, Mishra D D, Agarwala V & Mandal M K, *Mater Sci Semicond Process*, 16 (2013) 525.
9 Devi S & Srivastva M*, Indian J Phys,* 84 (2010) 1561.
10 Bhadra J & Sarkar D, *Indian J Phys,* 84 (2010) 693
11 Sharma G, Kumar A, Sharma S, Naushad Mu, Dwivedi R P, ALOthman Z A & Mola G T, *J King Saud Univ Sci,,* 31 (2019) 257.
12 Wang X, Chen C, Chang Y, Liu H, *J Hazard Mater*, 161 (2009) 815.
13 Laszlo Guczi, *Catal Today*, 101 (2005) 53.
14 Harada M & Cong C, *Ind Eng Chem Res*, 55 (2016) 5634.
15 Cortie M B & McDonagh A M, *Chem Rev*, 111 (2011) 3713.
16 Smith G B & Granqvist C G S, *Green nanotechnology: Solutions for sustainability and energy in the built environment*, (CRC Press, Boca Raton, FL, USA), 2010.
17 Tari F, Manteghian M & Tazarv S, *Int J Nanosci Nanotechnol,* 14 (2018) 57.
18 Kim H, Xuan H & Jack K, *Int J Mol Sci*, 21 (2020) 5174.
19 Matin A, Jang J H & Kwon Y U, *Int J Hydrog Energy*, 39 (2014) 3710.
20 Yeshchenko O A, Kozachenko V V & Tomchuk A V, *Surf Plasm Res*, 63 (2018) 386.
21 Qiao H, Wei Z, Yang H, Zhu L & Yan X, *J Nanomater,* 2009 (2009) Article ID 795928.
22 Mohammed M R, Khan S B, Jamal A, Mohd F & Abdullah M A, *Nanomaterials,* 63 (2018) 2071.
23 Liu Y & Shen X, *J Saudi Chem Soc*, 23 (2019) 1032.
24 Mohammadyani D, Hosseini S A & Sadrnezhaad S K, *Int J Mod Phys Conf Ser,* 5 (2012) 270.
25 Mishra A & Sardar M, *Nanotechnology,* 45 (2014) 309.
26 Gawande M B, Rathi A K, Branco P S, Nogueira I D, Velhinho A, Shrikhande J J, Indulkar U U, Jayaram R V, Ghumman C A A, Bundaleski N & Teodoro O M N D, *Chem Eur J*, 18 (2012) 12628.
27 Tsukimura K, Sasaki S & Kimizuka N, *Jpn J Appl Phys,* 36 (1997) 3609.
28 Rathore P S, Patidar R, Shripathi T & Thakore S, *Catal Sci Technol*, 5 (2015) 286.